

Magnetic properties in a partially oxidized nanocomposite of Cu-CuCl

Qi Li and Shi-Wei Zhang^{a)}

State Key Laboratory for Structural Chemistry of Unstable and Stable Species, College of Chemistry and Molecular Engineering, Peking University, Beijing 100871, P. R. China

Yan Zhang and Chinping Chen^{b)}

Department of Physics and State Key Laboratory for Mesoscopic Physics, Peking University, Beijing 100871, P. R. China

PACS : 75.75.+a, 81.07.-b

Abstract

The magnetism of a very thin AFM CuO over the surface of partially oxidized nanocomposites of Cu-CuCl, ~ 200 nm, has been investigated. The samples are characterized by x-ray diffraction (XRD), x-ray photoelectron spectroscopy (XPS), x-ray-excited Auger electron spectroscopy (XAES), transmission electron microscope (TEM) and magnetic measurements. The XRD, XPS, XAES and TEM analyses indicate that the composites have a core-shell structure, with the diamagnetic metal Cu in the core enclosed by a diamagnetic shell of cubic CuCl and Cu₂O. A little of Cu²⁺ is detected by XPS and XAES over the outer surface. The magnetic measurements, including the field-cooled/zero-field-cooled (FC/ZFC) magnetization and field dependent magnetization (M-H), confirm that the magnetism is directly associated with the AFM CuO on the outer surface, attributed to the uncompensated surface spins of Cu²⁺. More interestingly, the magnetic susceptibility is greatly enhanced by the existence of Cl⁻ anion, possibly due to the frustration effect of the impurity reducing the AFM ordering of CuO.

I. INTRODUCTION

The magnetic properties of nanoscaled particles (NP's) have attracted more and more attention due to both the unique magnetic properties and the potential technological applications.^{1, 2} In AFM NP's, the large surface/volume ratio makes the surface effects important to the magnetic behavior. It is well known that the surface spins in AFM NP's lead to enhanced magnetic moments and modified superparamagnetism.³⁻⁶ However, there is still no consensus on the origin of this behavior. Many detailed studies have been reported on the magnetic properties of AFM NP's, including NiO,^{7,8} CoO,^{9,10,11} ferritin,^{12,13} α -Fe₂O₃,^{14,15} and ferrihydrites.^{16,17}

The bulk CuO has been extensively studied due to its relation to high-T_c superconductors. Magnetic susceptibility,^{18,19} specific heat^{20,21} and neutron diffraction^{22,23} measurements on the bulk CuO have revealed that the magnetic transitions occur at $T_{N1} = 212$ K and $T_{N2} = 231$ K. Recently, some unique magnetic properties of CuO NP's from other transition-metal monoxides (such as NiO, CoO) have been reported,^{24,25} which are attributed to its different unit cell and the coordination style of copper with respect to oxygen. In this paper, we report a detailed investigation on the magnetic property of the partially oxidized nanocomposites of Cu-CuCl with a core-shell structure. The magnetism is evidenced to be related to the Cu²⁺ residing over the surface. It directly confirms that, indeed, the surface AFM CuO would exhibit ferrimagnetism. Also, the existence of Cl⁻ ions would modified the magnetic ordering of CuO, hence, greatly enhancing the magnetism.

II. SAMPLE

A typical sample was prepared by the following procedure: CuCl₂·6H₂O in water solution was reduced to metal Cu NP's at 80 °C by hydrazine hydrate. Afterwards, the unreacted hydrazine hydrate was washed away. A small amount of CuCl₂·6H₂O was then added to the solution to form a CuCl shell

enclosing the Cu NP's. Then, the Cu-CuCl composites were filtrated out, washed three times by ethanol, and dried in vacuum. The final product was obtained through controlled air oxidation of the Cu-CuCl composites powder at room temperature. During the process of synthesis, the CuCl shell is critical in order to obtain a sample with interesting magnetic properties, although the molar ratio of CuCl/Cu accounts for only 1 %.

The samples were analyzed by X-Ray diffraction (XRD) using a Rigaku diffractometer and CuK α radiation ($\lambda = 0.15418$ nm). The XRD patterns for the metal Cu, the Cu-CuCl nano-composites before and after the oxidation are plotted in Fig. 1. The crystalline grain size (D_{XRD}) was calculated from the width of the XRD peaks using the Scherrer relation after correcting for the instrumental broadening. It indicates that the composites are made up of cubic Cu ($D \approx 26.7$ nm), cubic Cu₂O ($D \approx 12.6$ nm) and cubic CuCl ($D \approx 24.8$ nm). A noteworthy point is that, after the oxidation, only the peak for Cu₂O shows up, while, there is not any detectable CuO within the detection sensitivity of XRD. XPS analysis was performed to determine the elements chemical state on the surface of the Cu-Cl composites before and after the oxidation, using an Axis Ultra spectrometer (Kratos, UK) with mono AlK α (1486.71 eV) radiation at a power of 225 w (15 mA, 15 kV). To compensate for the surface charge effects, binding energies were calibrated using C 1s hydrocarbon peak at 284.8 eV. As shown in Fig. 2, the curve for the sample before oxidation displays two symmetric peaks corresponding to the Cu 2p_{3/2} (932.6 eV) and Cu 2p_{1/2} (952.5 eV). On the other hand, in the curve for the oxidized sample, additional shoulders show up at positions, 934.6 eV and 954.7 eV, which are higher than the main peaks. These shoulders are owing to CuO²⁶. Furthermore, the accompanied shake-up satellite peaks approximately 9 eV higher than the shoulders are a signature for the Cu²⁺. The XPS analysis indicates that CuO appears after the oxidation, and exists on the surface of the NP. However, in consideration of the XRD result, the

amount is less than a few percent. X-ray-excited Auger spectrum (XAES) for the oxidized sample was recorded and shown in the inset of Fig. 2. The peak maximum of Cu L₃VV is at a kinetic energy of 916.3 eV (BE. 570.2 eV), agreeing with the literature value of Cu₂O. However, the peak shape is closer to that of CuO, confirming the existence of the Cu²⁺ on the surface²⁷. From the above analyses, including XRD, XPS, and XAES, the composites should be a complex, which has a core of Cu, a shell of CuCl and Cu₂O, along with a little Cu²⁺ locating on the surface. To confirm the structure of these composites, we have characterized them by TEM. Fig. 3a shows the TEM images of metal Cu nanoparticles. The particle size, ~ 200 nm, is much larger than the grain size calculated from XRD, indicating the polycrystalline structure within the NP. TEM image of the partially oxidized Cu-CuCl nanocomposites is shown in Fig. 3b. It reveals clearly the core-shell structure of the nanocomposites.

III. MAGNETIC MEASUREMENT

Magnetic properties of these composites in a powdered collection were measured using Quantum Design SQUID magnetometer. Temperature-dependent field-cooled (FC) and zero-field-cooled (ZFC) magnetic susceptibility, $\chi = M/H$, of a typical composite is shown in Fig. 4. The FC/ZFC curves exhibit a typical freezing behavior at a temperature below the blocking temperature, T_B , determined by the maximum in the ZFC curve. At $T < T_B$, the FC curve increases rapidly with decreasing temperature and becomes seventeen times the value of the ZFC one. Because the major composition of the samples is diamagnetic Cu, CuCl and Cu₂O, the only possible origin of the observed magnetism is from the small amount of CuO on the surface. The surface magnetism usually gives pronounced blocking effect due to the surface anisotropy or disorder state. The magnetic measurement is, therefore, in agreement with the sample characterization. At about 8 K, which is above T_B , the FC and ZFC curves collapse. The

susceptibility exhibits well-behaved Curie-Weiss law, $\chi \propto 1/(T+\theta)$. The inset (a) in Fig. 4 gives $\theta = 24.6$ K, for the sample with 30 days of oxidation. The Curie-Weiss parameter, θ , indicates the AFM nature of the spin interaction in the samples. The inset (b) in Fig. 4 shows the FC magnetic susceptibility of the samples with various oxidation time. It demonstrates that the samples with longer oxidation time exhibit larger magnetic susceptibility. This could be attributed to the higher Cu^{2+} content. The FC and ZFC magnetic susceptibility of the pellet and the powder samples were measured, also, as a function of temperature, shown in Fig. 5. The results show that χ of the pellet sample is much smaller than that of the powder one, especially at low temperature. It further confirms that the magnetic moments of these composites are coming from the surface.

Fig. 6 shows the FC susceptibilities with and without the CuCl . The sample with CuCl exhibits much higher value of FC susceptibility at $T < T_B$. For example, at 2 K, it is sixteen times the value of that without CuCl . This suggests that the existence of Cl^- tends to enhance the magnetism of CuO . The inset shows the ZFC data for both the samples. Likewise, the sample with the Cl^- has a much more pronounced susceptibility than the one without Cl^- . At $T = T_B$, the difference is about an order of magnitude.

The field dependence of the magnetization (M - H) curves were measured at 2 K, 6 K and 10 K, and plotted in Fig. 7. Below the blocking temperature, a hysteresis loop is observed, evidencing the existence of a ferromagnetism coming from the uncompensated surface spins of Cu^{2+} . The remanent magnetization and coercive field below T_B are $M_r = 0.124$ emu/g, $H_c = 5225$ Oe at 2 K and $M_r = 0.065$ emu/g, $H_c = 508$ Oe at 6 K. Above T_B , the M - H curve reveals a linear paramagnetic behavior, consistent with the result of FC/ZFC measurements. FC hysteresis loop was measured at 2 K under the cooling field of 30 kOe from 300 K down to 2 K. In Fig. 8, the FC hysteresis loop is slightly broadened,

however, remains symmetric about the origin like the ZFC one. There is no sign of any exchange bias, which is usually observed in the FM-AFM interface.^{11,28} This is consistent with the fact that Cu, CuCl, and Cu₂O underneath the surface are all diamagnetic.

IV. DISCUSSION

The FC/ZFC magnetic susceptibilities show that the composites have ferromagnetism at low temperature. The sample with longer oxidation time has higher magnetic susceptibility, resulting from the higher Cu²⁺ content. Along with the results of structure and composition characterizations, it provides a direct evidence that a thin layer of AFM CuO on the surface of a nano-sized diamagnetic core would exhibit FM property. The surface magnetism can be interpreted as owing to the uncompensated surface spins from the AFM CuO. More interestingly, however, the existence of the Cl⁻ anions would greatly enhance the magnetism below T_B. For samples with particle size of about 200 nm, 1 % of CuCl could almost enclose the entire copper core before oxidation. In the oxidation process, oxygen enters the sample from outside of the surface, becomes O²⁻ anions and oxidizes Cu⁺ cations (or metal Cu) into Cu²⁺. Then, a complex composed of Cu²⁺, Cl⁻, and O²⁻ forms on the surface of the composite. Besides CuO, minute CuCl₂ could likely appear during the oxidation process. The CuCl₂ and CuO are all AFM with different exchange constants, *J*, of 7 K²⁹ and 700 K³⁰, respectively. Therefore, the existence of Cl- is surely going to modify the superexchange interaction within the CuO by introducing the lattice distortion, impurity-induced frustration on the AFM ordering, etc. This is similar to the doping effect of Li into the CuO crystal³¹. The AFM magnetic ordering would be reduced. Thus, the magnetism is enhanced.

Usually, antiferromagnetic NP's are exchange biased, attributed to the FM-AFM coupling between the uncompensated surface spin layer and the antiferromagnetic core²⁴. Similarly, in the very

recent report¹¹, Bawendi et al did not find any exchange bias in the Co NP's with a thin shell, ~ 1 nm, of CoO, indicating that the very thin CoO layer does not exhibit AFM property. On the other hand, a thicker CoO layer, ~ 3.2 nm, has kept the AFM property to demonstrate the exchange bias effect. In our measurement, no exchange bias effect is observed, implying that the surface CuO is very thin to show only the ferromagnetism. This is in consistent with the characterization of XPS and XAES.

IV. CONCLUSIONS

In conclusion, the magnetism from the thin surface CuO layer has been investigated in the partially oxidized nanocomposites of Cu-CuCl. The ferromagnetism is from the uncompensated surface spin of Cu²⁺ in CuO. In addition, the existence of Cl⁻ would greatly enhance the magnetism, possibly by introducing the frustration effect into the AFM system of CuO. The M-H measurement at 2 K, under the FC of 30 kOe, gives Hc ~ 5700 Oe, without any exchange bias effect observed. This is consistent with the structure of a thin surface CuO enclosing a diamagnetic core, rather than an antiferromagnetic one. These materials are unique in the magnetic property of the AFM NP's and are helpful in understanding the nature of the magnetism about the AFM NP's.

ACKNOWLEDGMENT

This work was supported by NSFC of China (No. 20273001).

References

- a) e-mail: zhangsw@pku.edu.cn
 - b) e-mail: cpchen@pku.edu.cn
1. D. E. Speliotis, J. Magn. Magn. Mater. **193**, 29 (1999).
 2. R. H. Kodama and A. E. Berkowitz, Phys. Rev. **B 59**, 6321 (1999).
 3. J. T. Richardson and W. O. Milligan, Phys. Rev. **102**, 1289 (1956).

4. T. Takada and N. Kawai, *J. Phys. Soc. Jpn.* **17**, 691 (1962).
5. J. Cohen, K. M. Creer, R. Pauthenet and K. Srivastava, *J. Phys. Soc. Jpn.* **17**, 685 (1962).
6. W. J. Schuele and V. D. Deetscreek, *J. Appl. Phys.* **33**, 1136 (1962).
7. J. T. Richardson, D. I. Yiagas, B. Turk, K. Forster and M. V. Twigg, *J. Appl. Phys.* **79**, 6977 (1991).
8. S. A. Makhlof, F. T. Parker, F. E. Spada and A. E. Berkowitz, *J. Appl. Phys.* **81**, 5561 (1997).
9. I. V. Krivorotov, H. Yan, E. D. Dahlberg and A. Stein, *J. Magn. Magn. Mater.* **226-230**, 1800 (2001).
10. L. Zhang, D. Xue and C. Gao, *J. Magn. Magn. Mater.* **267**, 111 (2003).
11. J. B. Tracy, D.N. Weiss, D.P. Dinega, and M.G. Bawendi, *Phys. Rev. B* **72**, 064404 (2005)
12. S. A. Makhlof, F. T. Parker, F. E. Spada and A. E. Berkowitz, *Phys. Rev. B* **55**, R14 717 (1997).
13. S. Gider, D. D. Awschalom, S. Mann, and M. Chaparala, *Science* **268**, 77 (1995).
14. M. Vasquez-Mansilla, R.D. Zysler, C. Arciprete, M. Dimitrijewits, D. Rodriguez-Sierra, and C. Saragovi, *J. Magn. Magn. Mater.* **226**, 1907 (2001).
15. M. M. Ibrahim, J. Zhao, and M. S. Seehra, *J. Mater. Res.* **7**, 1856 (1992).
16. M. S. Seehra, V. S. Babu, A. Manivannan and J. W. Lynn, *Phys. Rev. B* **61**, 3513 (2000).
17. J. L. Jambor and J. E. Dutrizac, *Chem. Rev.* **98**, 2549 (1998).
18. T. I. Arbuzova, A. A. Samokhvalov, I. B. Smolyak, B. V. Karpenko, N. M. Chebotaev and S. V. Naumov, *J. Magn. Magn. Mater.* **95**, 168 (1991).
19. T. I. Arbuzova, I. B. Smolyak, A. A. Samokhvalov and S. V. Naumov, *J. Exp. Theor. Phys.*, **86**, 559 (1998)
20. J.W. Loram, K. A. Mirza, C. P. Joyce, A. J. Osborne, *Europhys. Lett.* **8**, 263 (1989).

21. D. D. Lawrie, J. P. Frank and C-T Lin, *Physica C* **297**, 59 (1998).
22. P. J. Brown, T. Chattopadhyay, J. B. Forsyth, V. Nunez and F. Tasset, *J. Phys. C: Condens. Matter* **3**, 4281 (1991).
23. M. Ain, A. Menelle, B. M. Wanklyn and E. F. Bertaut, *J. Phys. C: Condens. Matter* **4**, 5327 (1992).
24. A. Punnoose, H. Magnone and M. S. Seehra, *Phys. Rev. B* **64**, 174420 (2001).
25. R. A. Borzi, S. J. Stewart, R. C. Mercader, G. Punte and F. Garcia, *J. Magn. Magn. Mater.* **226-230**, 1513 (2001).
26. S. S. Chang, H. J. Lee and H. J. Park, *Ceram. Int.* **31**, 411 (2005). H.B. Tu and J.Q. Wang, *Poly. Degrad. Stabil.* **54**, 195 (1996)
27. S. Poulston, P. M. Parlett, P. Stone and M. Bowker, *Surf. Interface Anal.* **24**, 811 (1996).
28. See the reviews by A. E. Berkowitz and K. Takano, *J. Magn. Magn. Mater.* **200**, 552 (1999); J. Nogues and I. K. Schuller, *ibid.* **192**, 203 (1999).
29. L. J. de Jongh and A. R. Miedema, *Adv. Phys.* **23**, 1 (1974).
30. T. Shimizu, T. Matsumoto, A. Goto, T.V. Chandrasekhar Rao, K. Yoshimura, and K. Kosuge, *Phys. Rev. B* **68**, 224433 (2003)
31. X.G. Zhang, H. Yamada, D.J. Scanderbeg, M.B. Maple, and C.N. Xu, *Phys. Rev. B* **67**, 214516 (2003).

Figure captions

Figure 1. XRD patterns for the metal Cu, Cu-CuCl before oxidation, and partially oxidized Cu-CuCl. In the curve for the oxidized sample, only the peak for Cu_2O shows up. The CuO is beyond the detection sensitivity.

Figure 2. XPS data for the Cu-CuCl before and after the oxidation. The shoulders in the curve for the oxidized sample, slightly higher than the main peaks of $\text{Cu } 2\text{p}_{3/2}$ and $\text{Cu } 2\text{p}_{1/2}$, are the signature for Cu^{2+} . Inset is the $\text{Cu } \text{L}_3\text{VV}$ of XAES. The peak position agrees with the literature value of Cu_2O , while the peak shape is closer to that of CuO .

Figure 3. (a) TEM image of metal Cu nanoparticles.

(b) TEM image of partially oxidized Cu-CuCl nanocomposites. A shell structure in a lighter shade surrounding a dark core is obvious.

Figure 4. Temperature variation of the magnetic susceptibility, χ , under ZFC (zero-field-cooled) and FC (field-cooled) at 100 Oe of measurement field for the sample of 30 days oxidation. The blocking temperature, T_B , is 6.4K. Inset (a) shows the magnetic susceptibility χ exhibiting well-behaved Curie-Weiss law at $T > 70\text{K}$; inset (b) shows the magnetic susceptibility χ under FC of samples with different oxidation time, (1) 6 days, (2) 12 days, (3) 18 days, (4) 24 days, (5) 30 days, (6) 36 days, (7) 42 days. It indicates that the longer oxidation time with the samples, the larger the magnetic susceptibility.

Figure 5. Temperature variation of the magnetic susceptibility χ with the pellet and powder samples under ZFC (zero-field-cooled) and FC (field-cooled) measured at 90 Oe. The powder sample exhibits higher magnetic susceptibility by almost an order of magnitude than the pellet one.

Figure 6. Temperature variation of the FC magnetic susceptibility χ of the samples with and without

CuCl measured at 100 Oe. The oxidized Cu NP's was synthesized with the same oxidation time (36 days) as the one of oxidized Cu-CuCl. Inset is the ZFC magnetic susceptibility χ of both the samples. The FC magnetic susceptibility of the sample with Cl^- is higher than that without Cl^- by more than an order of magnitude.

Figure 7. Hysteresis loops of the powder sample at 2K, 6K and 10K with the cooling history of ZFC. Inset is for the loops in the low-field region. At 10 K, above the blocking temperature, the data is paramagnetic-like. While, at $T < T_B$, the loops indicate the existence of ferromagnetism.

Figure 8. Hysteresis loops of the powder sample at 2K with ZFC and FC at 30KOe. Inset is for the loops in the low-field region. No exchange bias effect is observed.

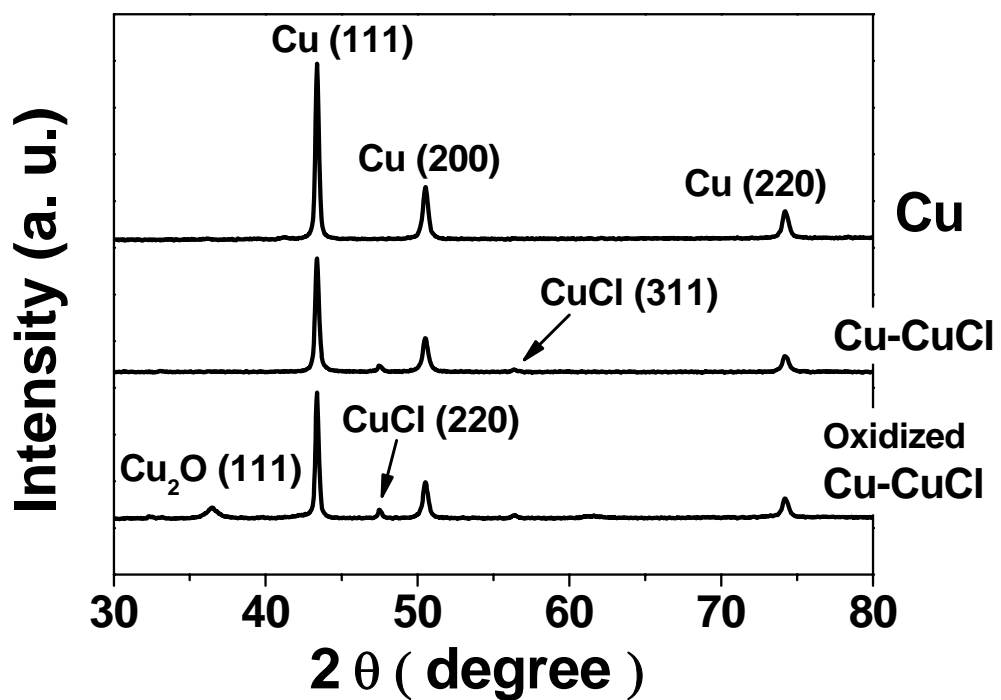


Figure 1.

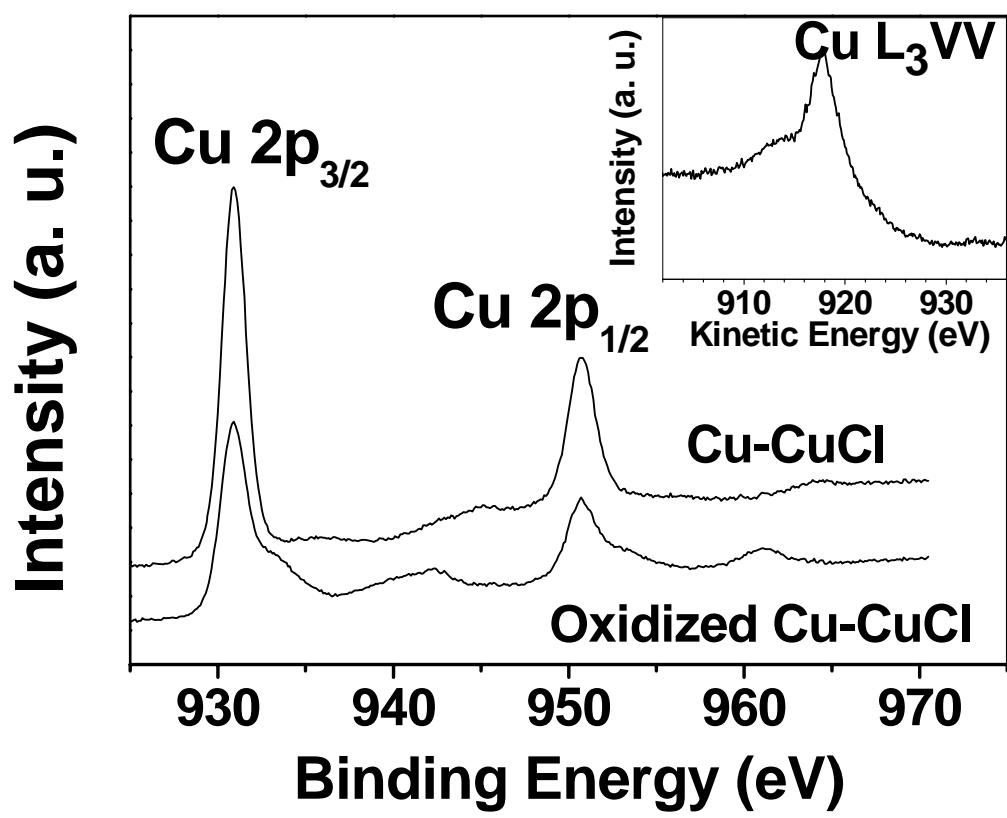


Figure 2.

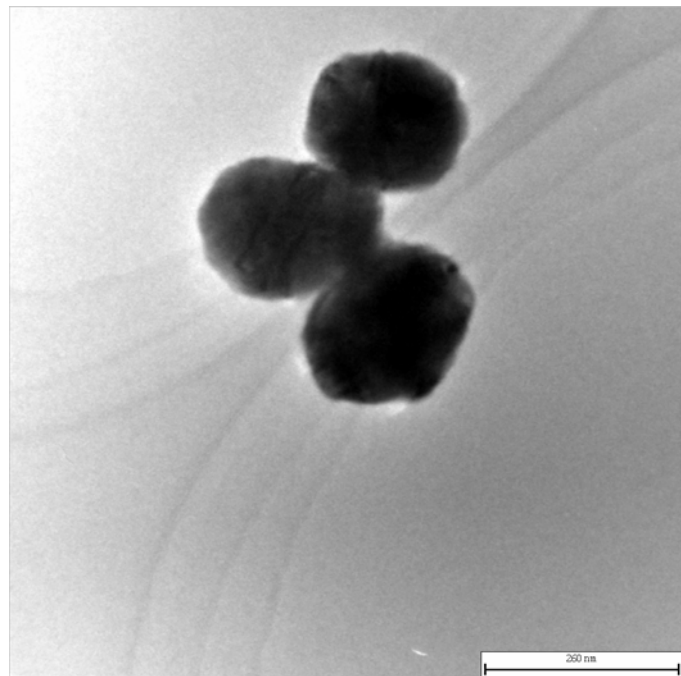


Figure 3a.

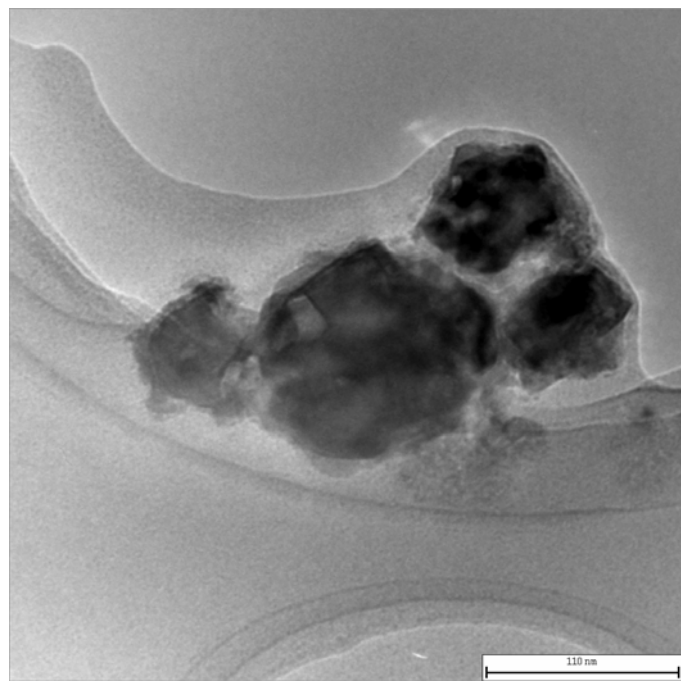


Figure 3b.

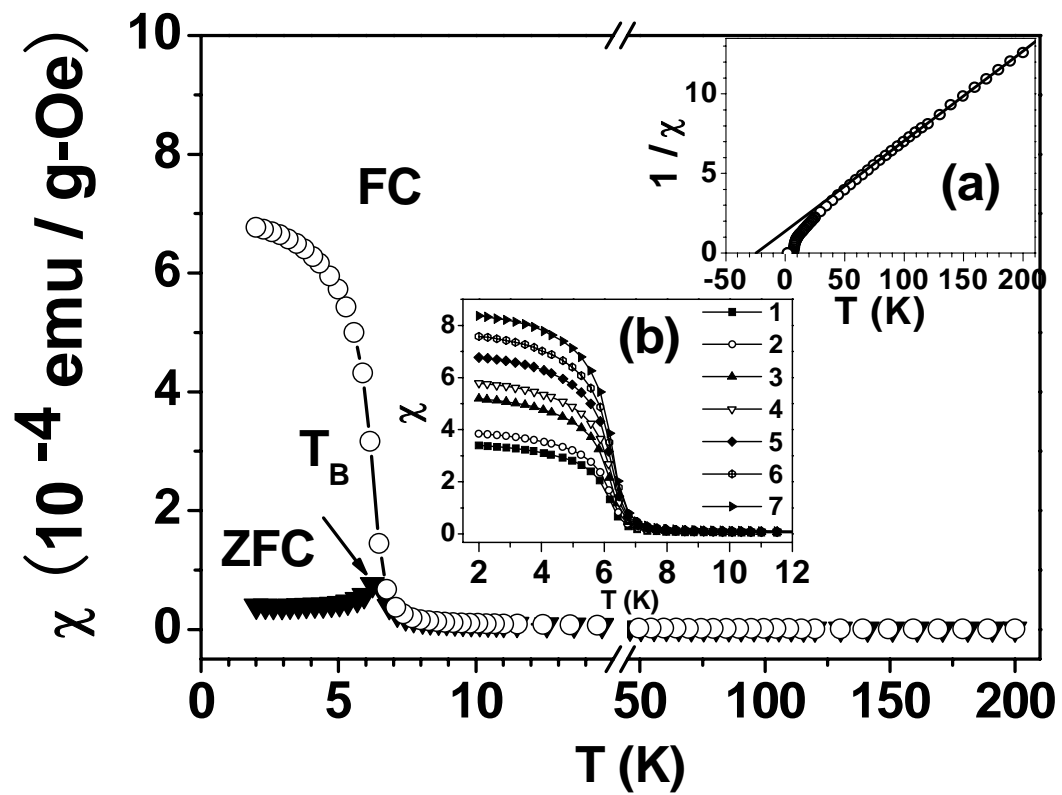


Figure 4.

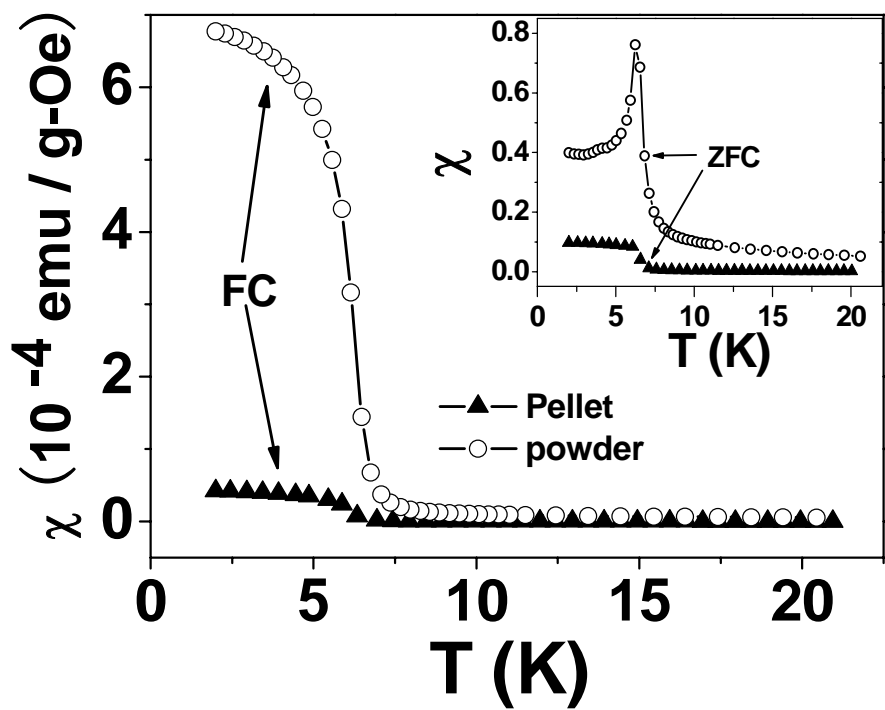


Figure 5.

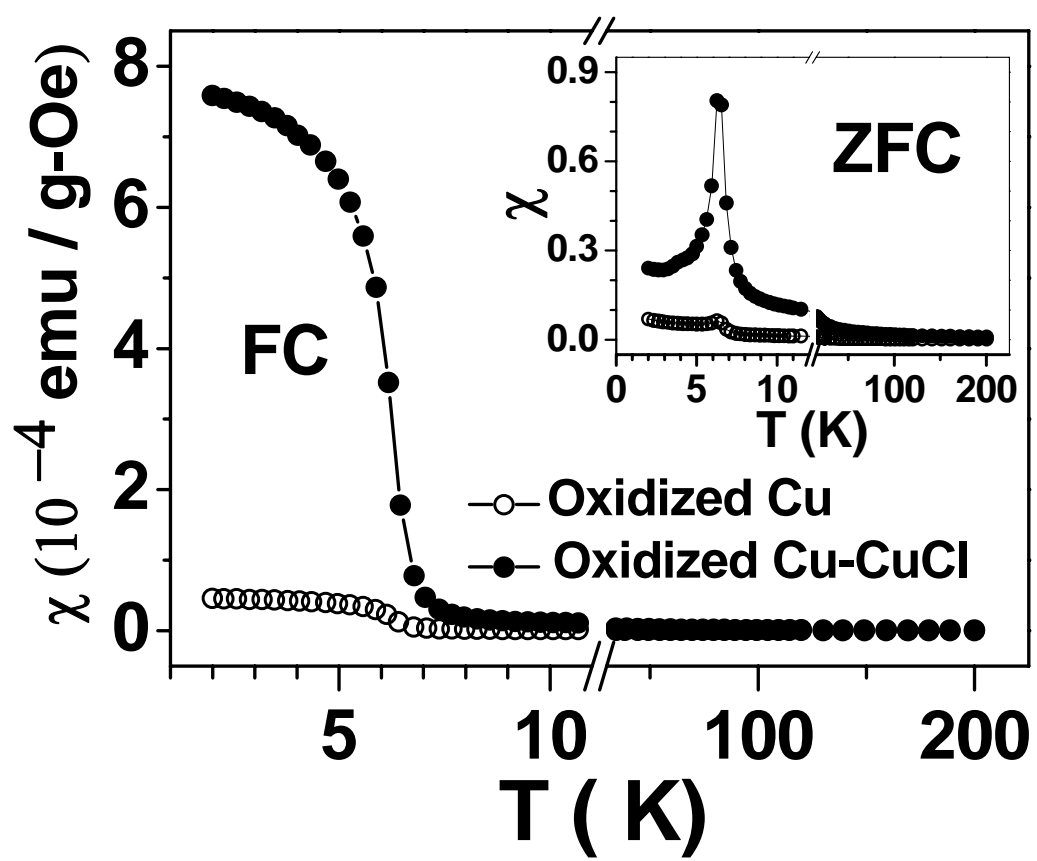


Figure 6.

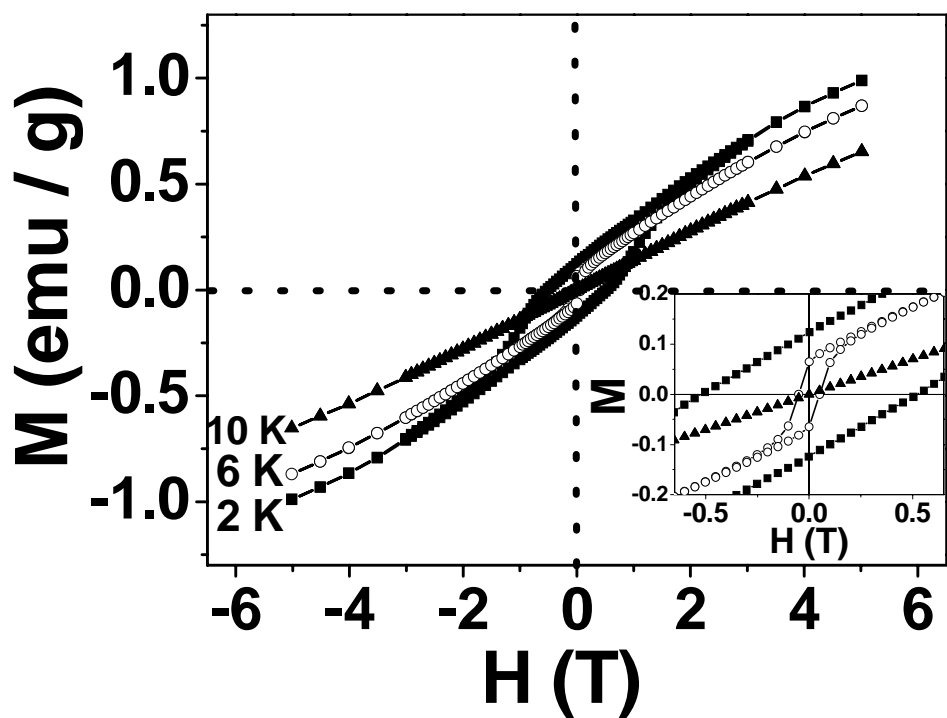


Figure 7.

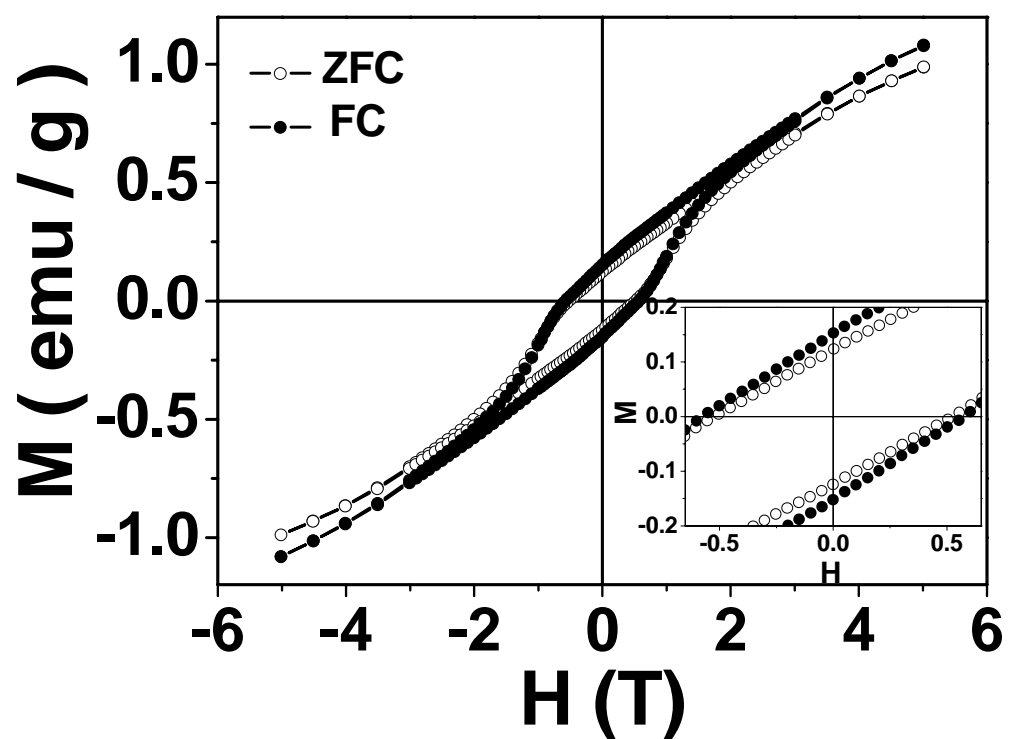


Figure 8.